WCDMA Uplink Capacity of a Long Tunnel Cigar-shaped Microcells for Underground Train Service

Bazil Taha-Ahmed · Miguel Calvo-Ramón · Leandro de Haro-Ariet

Abstract In this paper, the capacity and the interference statistics of the sectors of the cigar-shaped WCDMA microcells are studied using the hybrid model of propagation. A model of nine microcells in a metro tunnel is used to analyze the uplink capacity and the interference statistics. The capacity and the interference statistics of the microcells in metro tunnels are studied in this work for different propagation parameters, antenna side lobe levels, sector ranges and bends losses.

Keywords WCDMA · Uplink capacity · Shadowing · Hybrid model of propagation

1 Introduction

WCDMA systems are characterized as being interference-limited, so reducing the interference results in increasing the capacity. Three techniques are normally used to reduce the interference: power control (PC) which is essential in the uplink, voice activity monitoring and sectorization which, for instance, can easily increase the macrocell capacity by a factor of 2.2 using three sectors. It is well known that urban microcell shapes may approximately follow the street pattern and that it is possible to have cigar-shaped microcells This kind of microcells can be deployed along metro tunnels and are the subject of this paper. The conditions that describe the tunnel cigar-shaped microcells under this study are

- The number of directional sectors of the cigar-shaped microcell base station is two and a directional antenna is used in each sector.
- The sector has typically a range R in between 1 and 1.5 km.
- The train within the tunnel can reach an speed of up to 120 km/h.

The antenna radiation pattern of the sector and the cigar-shaped microcell are shown in Fig. 1.

In Min et al. studied the performance of the CDMA highway microcells. Hashem et al. studied in the capacity and the interference statistics for hexagonal macrocells using a propagation exponent of 4.0. In [4] Ahmed et al. studied the capacity and interference statistics of highway cigar-shaped microcells. Ahmed et al. studied in the capacity and interference statistics of tunnel cigar-shaped microcells using a modified two slope propagation model assuming uniform distribution of users, perfect power control and very high transmitted power ignoring the effect of the thermal noise of the receiver. In Ahmed et al. studied the capacity of the cigar-shaped microcells sectors in a long tunnel assuming uniform distribution of users, perfect power control and infinite transmitted power. Ahmed et al. studied in the capacity of the sectors in long tunnels assuming uniform distribution of users, imperfect power control and infinite transmitted power. the W-CDMA uplink capacity and interference statistics of cigar-shaped microcells in over-ground train service with imperfect power control and finite transmitted power have been studied. It has been shown that in this scenario the capacity is minimum when trains are in the midway between the base stations. the W-CDMA uplink practical capacity and interference statistics of rural highways cigar-shaped microcells with

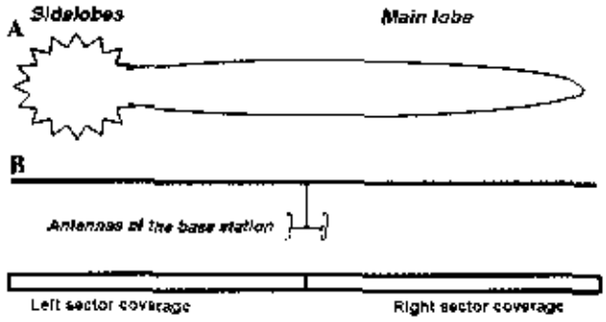

Fig. 1 Directional antenna radiation diagram (a) and microcell coverage (b)

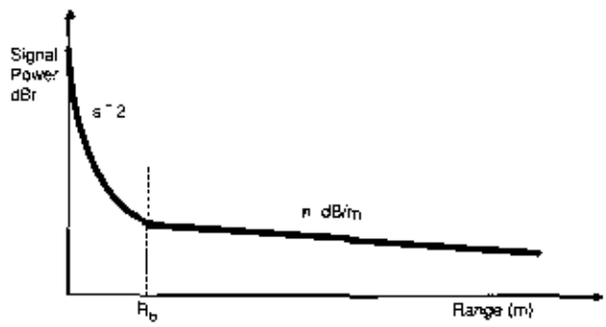

Fig. 2 Received power intensity profile

imperfect power control and finite transmitted power have been given where the two-slope model of propagation has been used to calculate the propagation loss. In [10], the WCDMA multiservice (voice and data) uplink capacity of highways cigar-shaped microcells has been studied.

In this work, we will use a nine cigar-shaped microcells model to study the capacity and interference statistics of the uplink in a WCDMA system where the hybrid propagation model is used. Here the users are not uniformly distributed within the microcells since they exist only within the metro trains.

The paper has been organized as follows. In Sect. 2, the hybrid propagation model is given. Section 3 explains the method to obtain the capacity and the interference statistics of the uplink. Numerical results are presented in Sect. 4. Finally, conclusions are drawn in Sect. 5.

2 Propagation Model

From the measurements presented the propagation model in the tunnels can be approximated by a two or more slopes model applicable in the microwave frequency range. A hybrid propagation model with lognormal shadowing is used in our calculations. The propagation exponent until the break point R_b is assumed to be s. For a distance r greater than R_b, the signal is assumed to be attenuated by a *specific attenuation factor of n dB/m. In this way the path* loss is given by:

$$L_p\,(\mathrm{dB}) = K + 10\log r^s + L_{\mathrm{glass}} + L_1 + \xi_1 \quad \text{If } r \le R_b \tag{1}$$

$$L_p\,(\mathrm{dB}) = K + 10\log R_b^s + n(r - R_b) + L_{\mathrm{glass}} + L_2 + \xi_2 \quad \text{If } r > R_b \tag{2}$$

where

- K is the attenuation at a distance of 1 m,
- s is the propagation exponent until R_b,
- n is the specific attenuation after R_b,
- L_{glass} is the insertion loss through the train windows and are assumed to be 4 dB,
- L_1 is the tunnel bend loss, if applicable, between the source and the observation point d,
- ξ_1 and ξ_2 are Gaussian random variables of zero-mean and standard deviations of σ_1 and σ_2, respectively.

For the tunnel environment, r is the distance between the base station of the microcell C and the mobile and the breakpoint distance R_b is given by:

$$R_b \approx \max\left(\frac{a^2}{\lambda}, \frac{b^2}{\lambda}\right) \tag{3}$$

where a is the tunnel height, b is the tunnel width and λ is the wavelength.

Typical value of s is 2 and the value of n is in between 0.01 and 0.02 dB/m [11] .

Figure 2 depicts the general shape of the propagation loss profile for the tunnel microcell.

3 *Uplink Analysis*

Figure 3 shows the configuration of the multi-microcells model. Each microcell controls the transmitted power of its users. The sector range is assumed to be R. If the interfering user i is at a distance r_{im} from the nearest base station and at a distance r_{id} from the microcell d, as shown in Fig. 4, then the normalized loss $L(r_{id}, r_{im})$, due to the distance and bends only, is given as:

- If (r_{id} and $r_{im} \le R_b$) then $L\,(r_{id}, r_{im})$ is

$$L(r_{id}, r_{im}) = \frac{10^{\left[10\log r_{im}^{s} + L_{bim}\right]/10}}{10^{\left[10\log r_{id}^{s} + L_{bid}\right]/10}} \tag{4}$$

- If $r_{id} > R_b$ and $r_{im} \le R_b$ then $L\,(r_{id}, r_{im})$ is

$$L(r_{id}, r_{im}) = \frac{10^{\left[10\log r_{im}^{s} + L_{bim}\right]/10}}{10^{\left[10\log R_b^{s} + n(r_{id} - R_b) + L_{bid}\right]/10}} \tag{5}$$

- If $r_{id} \le R_b$ and $r_{im} > R_b$ then $L\,(r_{id}, r_{im})$ is

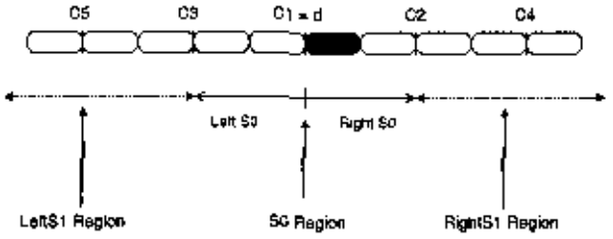

Fig. 3 Microcells model (only five microcells are shown)

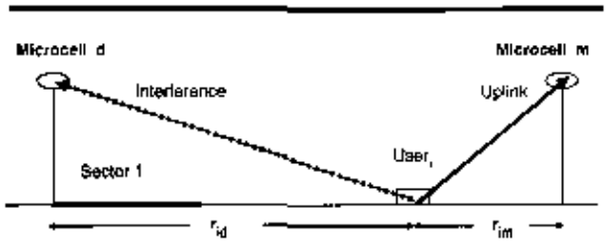

Fig. 4 Schematic diagram of base stations and mobiles for tunnel microcells

$$L(r_{id}, r_{im}) = \frac{10^{\left[10\log R_b^n + n(r_{im} - R_b) + L_{bm}\right]/10}}{10^{\left[10\log r_{id}^n + L_{bd}\right]/10}} \tag{6}$$

- If $r_{id} \leq R_b$ and $r_{im} > R_b$ then $L(r_{id}, r_{im})$ is

$$L(r_{id}, r_{im}) = \frac{10^{\left[n(r_{im} - R_b) + L_{bm}\right]/10}}{10^{\left[n(r_{id} - R_b) + L_{bd}\right]/10}} \tag{7}$$

where L_{bij} is the bend loss between the user i and the base station j.

Now the normalized loss $L_{shd}(r_{id}, r_{im})$ due to the distance, the bends and shadowing is given by:

$$L_{shd}(r_{id}, r_{im}) = 10^{(\xi_{id} - \xi_{im})/10} L(r_{id}, r_{im}) \tag{8}$$

ξ_{id} and ξ_{im} are given as:

- In case of (r_{id} and $r_{im} \leq R_b$) then $\xi_{id} = \xi_1$ and $\xi_{im} = \xi_1$.
- If $r_{id} > R_b$ and $r_{im} \leq R_b$ then $\xi_{id} = \xi_2$ and $\xi_{im} = \xi_1$.
- When $r_{id} \leq R_b$ and $r_{im} > R_b$ then $\xi_{id} = \xi_1$ and $\xi_{im} = \xi_2$.
- In case of (r_{id} and $r_{im} > R_b$) then $\xi_{id} = \xi_2$ and $\xi_{im} = \xi_2$.

In order to calculate the sector capacity, we have to calculate the expected value and the variance of the interference. Interference could be intracellular, due to the users in the sector under study, or intercellular, due to the users in other sectors.

We will divide the total intercellular interference (I_{inter}) into the interference from users in the $S0$ region (I_{S0}) and the interference from users in the $S1$ region (I_{S1}), where these regions are shown in Fig. 3. We will find the interference at the right sector (drawn in blank) of the central microcell C1 assuming it to be the microcell d. Users in the regions $S0$ and $S1$ are assumed to communicate with the best (with lower propagation loss) of the two nearest microcells. Thus, users within the $S1$ zone will not communicate with the microcell under study and their signals will always behave as an intercellular interference.

Let the power level of desired signal received at the base station be P_r. The interference from an active user communicating with the home microcell will be also P_r. A user i in the $S0$ region will not communicate with the home base station d, but rather with the base station m, if $\phi(\xi_{id} - \xi_{im}, r_{id}/r_{im}) = 1$, where

$$\phi(\xi_{id} - \xi_{im}, r_{id}/r_{im}) = \begin{cases} 1, & \text{if } L(r_{id}, r_{im}) 10^{(\xi_{id} - \xi_{im})/10} \leq 1 \\ 0, & \text{otherwise.} \end{cases} \tag{9}$$

Assuming a uniform density of users within the train that has a length of L_{train}, the density of users in each sector is $\rho = N_u / L_{train}$ users per unit length. If the activity factor of the user is α, then for the right part of $S0$ the expected value of I_{S0} is given as:

$$E[I_{S0}]_r = \alpha\rho \int_{S0r} L(r_{id}, r_{im}) f\left(\frac{r_{id}}{r_{im}}\right) U(r)\, dr \tag{10}$$

where

$$f\left(\frac{r_{id}}{r_{im}}\right) = E\left[10^{(\xi_{id} - \xi_{im})/10} \phi(\xi_{id} - \xi_{im}, r_{id}/r_{im})\right] \tag{11}$$

$$= e^{(\beta\sigma)^2/2} Q\left[\beta\sigma - \frac{10}{\sigma}\log_{10}\{1/L(r_{id}, r_{im})\}\right] \tag{12}$$

where $\beta = (\ln 10)/10$ and $U(r)$ is an indication function given as

$$U(r) = \begin{cases} 1, & \text{if the train exists.} \\ 0, & \text{otherwise.} \end{cases} \tag{13}$$

Now the value of σ^2 is given as:

- When (r_{id} and $r_{im} \leq R_b$) then $\sigma_{id} = \sigma_1$, also $\sigma_{im} = \sigma_1$ then

$$\sigma^2 = 2(1 - C_{dm})\sigma_1^2 \tag{14}$$

where C_{dm} is the inter-sites (base stations) correlation coefficient of shadowing.

- If $r_{id} \leq R_b$ and $r_{im} > R_b$ or $r_{id} > R_b$ and $r_{im} \leq R_b$ then the value of σ^2 is given by

$$\sigma^2 = (\sigma_1 - \sigma_2)^2 + 2(1 - C_{dm})\sigma_1\sigma_2 \tag{15}$$

- When (r_{id} and $r_{im} > R_b$) then $\sigma_{id} = \sigma_2$, also $\sigma_{im} = \sigma_2$ then

$$\sigma^2 = 2(1 - C_{dm})\sigma_2^2 \tag{16}$$

$Q(x)$ is given by

$$Q(x) = \frac{1}{\sqrt{2\pi}} \int_{x}^{\infty} e^{-v^2/2} dv \tag{17}$$

The expected value of I_{S1} due to right part of the $S1$ region is given as

$$E[I_{S1}]_r \approx \alpha\rho \int_{S1r} L(r_{id}, r_{im}) E\left[10^{(\xi_{id}-\xi_{im})/10}\right] U(r) dr \tag{18}$$

The expected value of the intercellular interference from the right side of the regions $S0$ and $S1$ is

$$E[I]_r = E[I_{S0}]_r + E[I_{S1}]_r \tag{19}$$

For the left part of the sector under consideration, interference is injected through the back lobe (Sll) of the antenna of the sector under consideration. Thus, for the left part of $S0$ the expected value of I_{S0} is given as:

$$E[I_{S0}]_l \approx \alpha\, \rho\, Sll \int_{S0l} L(r_{id}, r_{im})\, f\left(\frac{r_{id}}{r_{im}}\right) U(r)\, dr \tag{20}$$

where Sll is the side lobe level (back lobe) of the directional antenna used in each sector.

The expected value of I_{S1} due to the left part of $S1$ is given as:

$$E[I_{S1}]_l \approx \alpha\rho Sll \int_{S1l} L(r_{id}, r_{im}) E\left[10^{(\xi_{id}-\xi_{im})/10}\right] U(r) dr \tag{21}$$

Then the expected value of the intercellular interference from the left side of the regions $S0$ and $S1$ is

$$E[I]_l = E[I_{S0}]_l + E[I_{S1}]_l \tag{22}$$

And the expected value of the total interference from the left and right sides is given as

$$E[I]_{\text{inter}} = E[I]_r + E[I]_l \tag{23}$$

Finally, the expected value of the total intercellular interference power is given as

$$E[P]_{\text{inter}} = P_r E[I]_{\text{inter}} \tag{24}$$

And the expected value of the intracellular interference power is given by

$$E[P]_{\text{intra}} \approx \alpha P_r N_u (1 + Sll) \tag{25}$$

Taking into account an imperfect power control with standard deviation error of σ_c (dB), the total expected interference power P_r will be:

$$E\left[P_{\text{intf}}\right]_r = e^{\beta^2\sigma_c^2/2}(E[P]_{\text{intra}} + E[P]_{\text{inter}}) \tag{26}$$

In the uplink only $\varepsilon\, P_r$ of P_r is used in the demodulation (being $\varepsilon = 14/16 = 0.875$ or $\varepsilon = 15/16 = 0.9375$). Thus, the expected value of the uplink carrier-to-interference ratio $(C/I)_{\text{up}}$ is given as

$$E(C/I)_{\text{up}} = \frac{\varepsilon P_r}{E\left[P_{\text{intf}}\right]_r + N_r} \tag{27}$$

And the expected value of bit energy to the noise power density $(E_b/N_o)_{\text{up}}$ is given by:

$$(E_b/N_o)_{\text{up}} = E(C/I)_{\text{up}}\, G_p \tag{28}$$

where N_r is the base station receiver thermal noise and G_p is the WCDMA processing gain.

For a user with a bit rate less than 15 kbit/s and moving with an speed of 120 km/h, the $(E_b/N_o)_{\text{up}}$ ratio has to be 7 dB [12] . The expected number of users $E(N_u)$ is calculated based on (28).

The intercellular interference variance of I_{S0} due to right part of $S0$ is given as

$$\text{var}[I_{S0}]_r = \rho \int_{S0r} [L(r_{id}, r_{im})]^2 \times \left\{ p\alpha g\left(\frac{r_{id}}{r_{im}}\right) - q\alpha^2 f^2\left(\frac{r_{id}}{r_{im}}\right) \right\} U(r) dr \tag{29}$$

where

$$g\left(\frac{r_{id}}{r_{im}}\right) = E\left[10^{(\xi_{id}-\xi_{im})/10} \phi(\xi_{id} - \xi_{im}, r_{id}/r_{im})\right]^2 \tag{30}$$

$$= e^{2(\beta\sigma)^2} Q\left[2\beta\sigma - \frac{10}{\sigma}\log_{10}[1/L(r_{id}, r_{im})]\right] \tag{31}$$

$$p = e^{2\beta^2\sigma_c^2} \tag{32}$$

$$q = e^{\beta^2\sigma_c^2} \tag{33}$$

The intercellular interference variance of I_{S1} due to right part of $S1$ is given as

$$\text{var}[I_{S1}]_r \approx \rho \int_{S1r} [L(r_{id}, r_{im})]^2 \left\{ p\alpha E\left[(10^{(\xi_{id}-\xi_{im})/10})^2\right] - q\alpha^2 E^2\left[10^{(\xi_{id}-\xi_{im})/10}\right] \right\} U(r)\, dr \tag{34}$$

The intercellular interference variance of I_{S0} due to left part of $S0$ is given as

$$\text{var}[I_{S0}]_l = \rho Sll \int_{S0l} [L(r_{id}, r_{im})]^2 \times \left\{ p\alpha g\left(\frac{r_{id}}{r_{im}}\right) - q\alpha^2 f^2\left(\frac{r_{id}}{r_{im}}\right) \right\} U(r) dr \tag{35}$$

The intercellular interference variance of I_{S1} due to left part of $S1$ is given as:

$$\text{var}[I_{S1}]_l \approx \rho\, Sll \int_{S1l} [L(r_{id}, r_{im})]^2 \left\{ p\alpha E\left[(10^{(\xi_{id}-\xi_{im})/10})^2\right] - q\alpha^2 E^2\left[10^{(\xi_{id}-\xi_{im})/10}\right] \right\} U(r) dr \tag{36}$$

Thus the total intercellular interference variance due to the total region $S0$ and $S1$ is given by

$$\mathrm{var}[I]_{\mathrm{inter}} = \{\mathrm{var}[I_{S0}]_r + \mathrm{var}[I_{S1}]_r\} + \{\mathrm{var}[I_{S0}]_t + \mathrm{var}[I_{S1}]_t\} \tag{37}$$

The intracellular interference variance is given by

$$\mathrm{var}[I]_{\mathrm{intra}} \approx N_u(1 + SII)(p\alpha - q\alpha^2) \tag{38}$$

The total variance of the interference is calculated as

$$\mathrm{var}[I]_t = \mathrm{var}[I]_{\mathrm{inter}} + \mathrm{var}[I]_{\mathrm{intra}} \tag{39}$$

The total interference power variance is given by:

$$\mathrm{var}\left[P_{\mathrm{inf}}\right]_t = P_r^2 \mathrm{var}[I]_t \tag{40}$$

Finally, the outage probability P_{out} is calculated as:

$$P_{\mathrm{out}} = Q\left[\frac{E(I)_t\big|_{N_u=N_u} - E(I)_t\big|_{N_u=N}}{\sqrt{\mathrm{var}(I)_t\big|_{N_u=N}}}\right] \tag{41}$$

The F factor is calculated as

$$F = \frac{\text{Intercellular Interference}}{\text{Intracellular Interference}} = \frac{E[P]_{\mathrm{inter}}}{E[P]_{\mathrm{intra}}} \tag{42}$$

The effective interference power is given by:

$$\left[P_{\mathrm{inf}}\right]_{\mathrm{eff}} = E\left[P_{\mathrm{inf}}\right]_t + \gamma\left\{\sqrt{var\left[P_{\mathrm{inf}}\right]_t}\right\} \tag{43}$$

where γ is the deviation factor which is a function of the accepted outage probability. The practical value of γ is 2.05 (for an outage of 2%) to 2.35 (for an outage of 1%).

4 Numerical Results

In our estimation it has been assumed that the WCDMA processing gain $G_p = 256$ (voice service). For our calculations some reasonable figures are applied. The azimuth side lobe level is assumed to be -15 dB, the correlation coefficient $C_{dm} = 0.5$, $s_1 = 2$, $n = 1$ dB/100 m, $\sigma_1 = 2$ dB, $\sigma_2 = 2$ dB, $\sigma_c = 1.5$ dB, $\varepsilon = 0.9375$, $R_b = 250$ m and $R = 1000$ m unless other values are mentioned. The train length L_{train} is assumed to be 60 m. We assume that the accepted outage probability is 1% and that the capacity of the sectors is calculated at this probability. Also it is assumed that the base station antenna gain is 14 dB and that the thermal noise is -102 dBm for the base station receiver.

Firstly, we study the case of the voice service assuming a voice activity factor of 0.67 and a maximum transmitted power by the mobile of 23 dBm. Figure 5 shows the outage probability of the sector for the worst case (users within the train are in the midway between base stations). The sector capacity is 30 voice users. Figure 6 shows the outage probability of the sector for the best case (users are very near to the microcells base station). The sector capacity is 58 voice users.

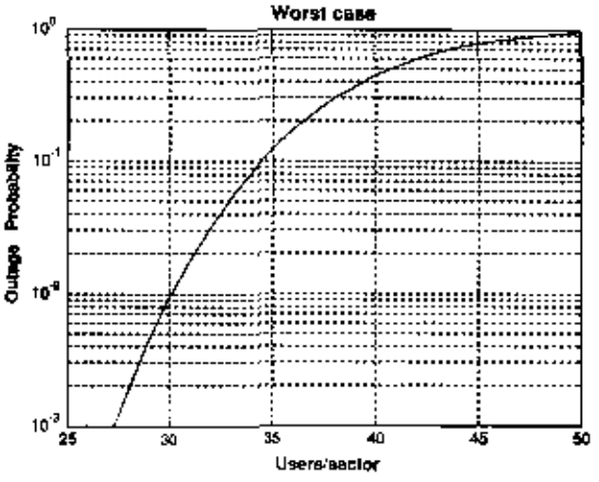

Fig. 5 Worst case outage probability of the sector

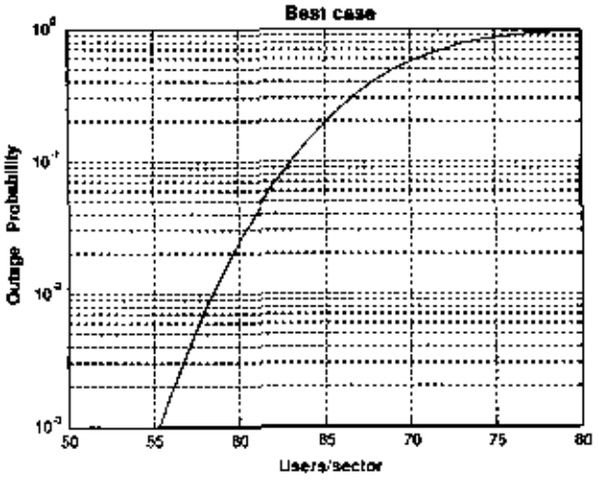

Fig. 6 Best case outage probability of the sector

Then we study the effect on the sector capacity of changing the attenuation factor n assuming n to vary between 1 and 2 dB/100 m. These values represent the lower and upper practical values of attenuation factor. Figure 7 shows the change of the worst case capacity with respect to n. We can notice that, the sector capacity increases when n increases.

The effect of the sector range on the sector capacity, for the worst case, is represented in Fig. 8 for two different values of n. It is noticed that, for $n = 1$ dB/100 m, the sector capacity increases with the increase of the sector range when it is lower than 1,500 m. For a sector range between (1,500 and 4,000) m, the sector range is almost constant. For a sector range higher than 4,000 m, the capacity reduces with the increase of the sector range. For $n = 2$ dB/100 m, the maximum sector capacity is obtained

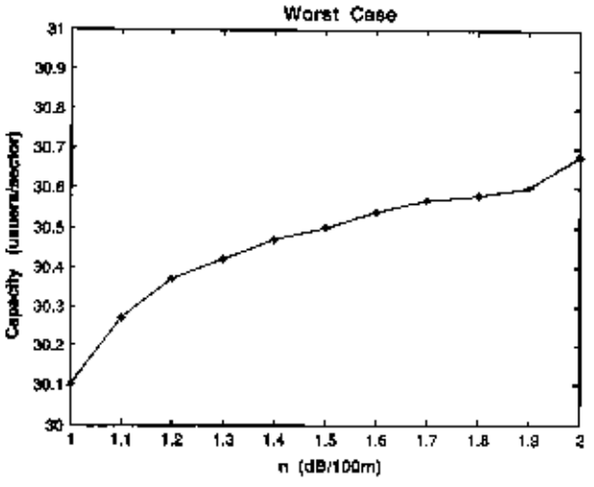

Fig. 7 Sector capacity as a function of n for $R = 1{,}000$ m

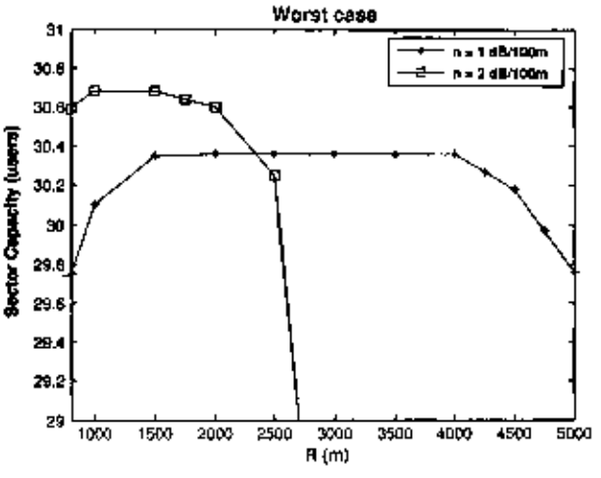

Fig. 8 Sector capacity as a function of the sector range R for two different n

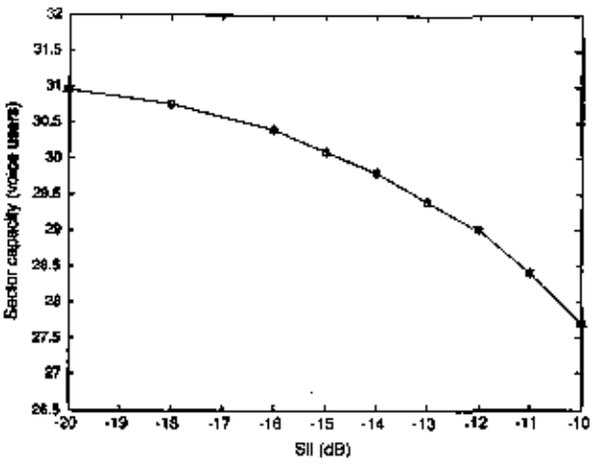

Fig. 9 Sector capacity as a function of side lobe level (for the worst case)

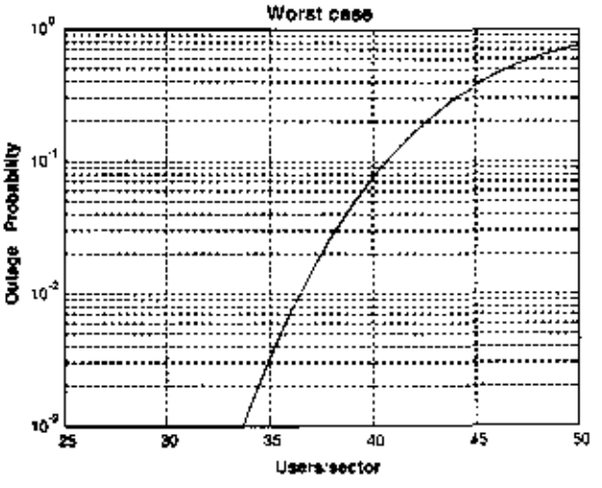

Fig. 10 Worst case sector performance with $L_{b12} = 3$ dB

when the sector range is in the order of 1,000–1,500 m. Practical sector range is in between 1 and 1.5 km, which is half the distance between two metro stations.

The effect of the side lobe level on the worst case sector capacity is depicted in Fig. 9. We can notice that reducing the side lobe level increases the sector capacity. An antenna with side lobe level lower than -15 dB is used.

Now we study the case when the bend losses $L_b \neq 0$ dB. We assume that there is a bend between microcell 1 and microcell 2 with a loss of 3 dB. Figure 10 shows the sector performance for the worst case. The sector capacity is 36 voice users. Thus, the sector capacity will be higher whenever the bend losses increases.

Finally, we study the case of data users assuming that the bit rate is 144 kbps, the required E_b/N_o is 2.8 dB [12] and the maximum transmitted power by the data mobile transmitter is 28 dBm. Figure 11 shows that the worst case sector capacity is four data users.

Figure 12 gives the worst case mixed capacity of the sector when we assume simultaneous voice and data users. It can be noticed an inverse linear relation, between the data capacity and the voice capacity.

Figure 13 depicts the locations of the trains for the worst case and best case. In practice, the sustained sector capacity is little bit more than the worst case capacity since the probability to be in this very bad situation is low.

5 Conclusions

We have presented a model that gives the capacity and interference statistics of an underground tunnel

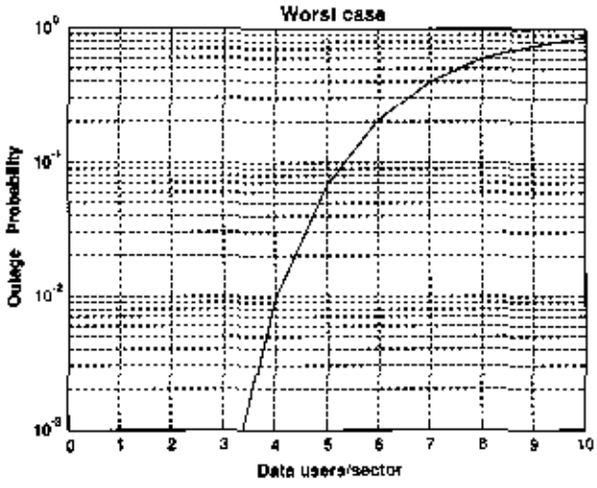

Fig. 11 Worst case sector performance for data service

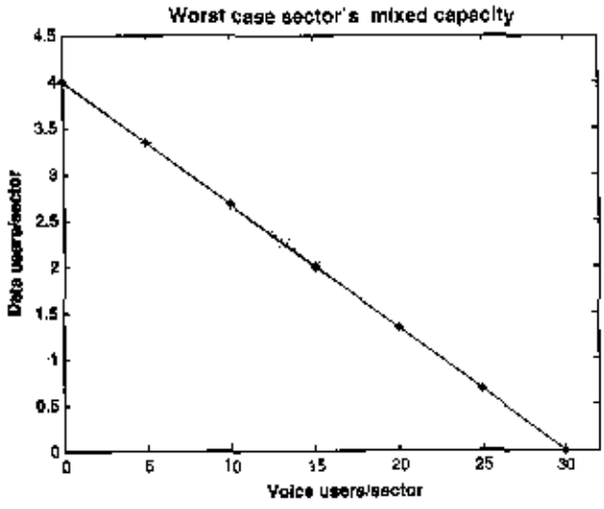

Fig. 12 Worst case mixed capacity of the sector

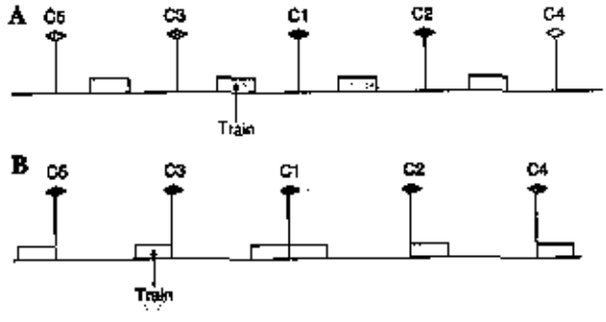

Fig. 13 Worst case and best case trains locations (a) Worst case (b) Best case

cigar-shaped microcells WCDMA system. The capacity of a sector is studied using a hybrid propagation model with lognormal shadowing and bend loss. The effect of the side lobe level of the directional antenna has been studied. Also, the effect on the sector capacity of the train position is studied where we can distinguish between two extreme cases (the best and the worst one case).

It has been noticed that

- With an antenna side lobe level of -15 dB, the capacity is almost the maximum possible.
- For a sector range between 1 and 1.5 km, the sector capacity is almost the maximum.
- Higher bend losses increases the sector capacity.
- Although results are not given, we have noticed also that increasing σ_1 and σ_2 reduces the sector capacity.

References

H.-S. Cho, M. Y. Chung, S. H. Kang, and D. K. Sung, Performance analysis of cross- and cigar-shaped urban microcells considering user mobility characteristics, *IEEE Vehicular Technology*, Vol. 49, No. 1, pp. 105–115, 2000.

S. Min and H. L. Bertoni, Effect of path loss model on CDMA system design for highway microcells, In *48th VTC*, Ottawa, Canada, pp. 1009–1013, May 1998.

B. Hashem and E. S. Sousa, Reverse link capacity and interference statistics of a fixed-step power-controlled DS/CDMA system under slow multipath fading, *IEEE Transactions on Communications*, Vol. 47, pp. 1905–1912, 1999.

B. Taha-Ahmed, M. Calvo-Ramón, and L. Haro-Ariet, Shaped W-CDMA cells performance in highways, *IJECE*, Vol. 1, No. 2, pp. 80–84, 2002.

B. Taha-Ahmed, M. Calvo-Ramón, and L. Haro-Ariet, W-CDMA uplink capacity and interference statistics of a long tunnel cigar-shaped microcells, *Journal of Communications and Networks*, Vol. 6, No. 2, pp. 106–111, 2004.

B. Taha-Ahmed and M. Calvo-Ramón, On the W-CDMA uplink capacity and interference statistics of a long tunnel cigar-shaped microcells, *Journal of Microwave and Optoelectronics*, Vol. 3, No. 3, pp. 28–40, 2003.

B. Taha-Ahmed, M. Calvo-Ramón, and L. Haro-Ariet, W-CDMA uplink capacity and interference statistics of a long tunnel cigar-shaped microcells using the hybrid model of propagation with imperfect power control, *Wireless Personal Communications*, Vol. 31, pp. 19–31, 2004.

B. Taha-Ahmed and M. Calvo-Ramón, W-CDMA uplink capacity and interference statistics of cigar-shaped microcells in over-ground train service with imperfect power control and finite transmitted power, *Wireless Personal Communications*, Vol. 43, No. 2 , pp.725–735, 2007.

B. Taha-Ahmed, M. Calvo-Ramón, and L. Haro-Ariet, W-CDMA uplink practical capacity and interference statistics of rural highways cigar-shaped microcells with imperfect power control and finite transmitted power, *Wireless Personal Communications*, Vol. 41, No. 1, pp. 43–55, 2007.

B. Taha-Ahmed and M. Calvo-Ramon, WCDMA multiservice uplink capacity of highways cigar-shaped microcells, *EURASIP Journal on Wireless Communications and Networking*, Vol. 2007, Article ID 84835, 8 pp., 2007.

Y. P. Zhang, A hybrid model for propagation loss prediction in tunnels, In *Millennium Conference on Antennas & Propagation*, Davos, Switzerland, April 2000.
B. Melis and G. Romano, UMTS W-CDMA: Evaluation of radio performance by means of link level simulations, *IEEE Personal Communications*, Vol. 7, No. 3, pp. 42–49, 2000.